A Kinetic Description of Dioxygen Motion within α- and β-Subunits of Human Hemoglobin in the R-State: Geminate and Bimolecular Stages of the Oxygenation Reaction

4 AUTHORS, INCLUDING:

Sergei V Lepeshkevich
National Academy of Sciences of Belarus
20 PUBLICATIONS **124** CITATIONS

SEE PROFILE

Jerzy Karpiuk
Polish Academy of Sciences
28 PUBLICATIONS **416** CITATIONS

SEE PROFILE

Igor Sazanovich
The University of Sheffield
46 PUBLICATIONS **903** CITATIONS

SEE PROFILE

A Kinetic Description of Dioxygen Motion within α- and β-Subunits of Human Hemoglobin in the R-State: Geminate and Bimolecular Stages of the Oxygenation Reaction[†]

Sergei V. Lepeshkevich,[‡] Jerzy Karpiuk,[§] Igor V. Sazanovich,[‡] and Boris M. Dzhagarov[*,‡]

Institute of Molecular and Atomic Physics, National Academy of Sciences of Belarus, 70 F. Skaryna Ave., Minsk 220072, Belarus, and Institute of Physical Chemistry, Polish Academy of Sciences, 01-224 Warsaw, Kasprzaka 44/52, Poland

ABSTRACT: Laser flash photolysis technique is used to study human hemoglobin (HbA) oxygenation. Monomolecular geminate oxygenation of triliganded R-state HbA molecules is described by a function of three exponentials. Geminate oxygenation of the α-subunit within R-state HbA is characterized by two components with time constants of 0.14 and 1 ns, while geminate oxygenation of the β-subunit within HbA is characterized by two components with time constants of 1 and ∼30 ns. Bimolecular oxygenation of triliganded R-state HbA molecules is described by a biexponential law. Two observed rate constants are assigned to oxygenation of the α- and β-subunit within HbA. The bimolecular association rate constants for O_2 rebinding with the α- and β-subunit within triliganded R-state HbA are $k_\alpha = 18.8 \pm 1.3$ $(\mu M \cdot s)^{-1}$ and $k_\beta = 52 \pm 4$ $(\mu M \cdot s)^{-1}$, respectively. The apparent quantum yields of photodissociation of the β- and α-subunit within completely oxygenated R-state HbA differ from each other by a factor of 3.6 and are equal to 0.041 ± 0.004 and 0.0114 ± 0.0012, respectively. The apparent quantum yield of photodissociation of completely oxygenated R-state HbA is equal to 0.026 ± 0.003.

Tetrameric human hemoglobin (HbA)[1] is an allosteric protein that carries molecular oxygen (O_2) in blood and tissues. With its relatively simple structure, it serves as a good model for studying nonlinear and cooperative interactions in proteins composed of several subunits. HbA is an ensemble of two dimers formed by a pair of α- and β-subunits, each containing heme b. This protein is known to be able to bind four O_2 molecules, one molecule per one heme in each subunit (*1*). With the use of X-ray diffraction analysis, it has been found that there exist two conformations of the HbA quaternary structure. Oxygenated HbA has a high-affinity structure called R (R-state), and the deoxygenated one has a low-affinity structure called T (T-state) (*1*). As HbA is oxygenated, its O_2 affinity is enhanced, and consequently, the protein itself regulates the ligand affinity (*1*, *2*). Since the α- and β-subunits differ in structure, knowledge of individual properties of each subunit type in the isolated state and in the different conformational forms of tetrameric HbA (*2−4*) is necessary to understand the molecular mechanism of HbA cooperative oxygenation.

Studies of photodissociation of the oxygenated protein (*5−21*) aimed to examine the dynamics of O_2 motion within the protein. This will make it possible to define O_2 trajectories when the molecular oxygen moves in the interior of the protein toward the binding center and when it moves back to the surrounding medium. The considered motion is a complex process. It is commonly accepted that after photodissociation, a free O_2 molecule moves diffusionally inside the protein globule, successively overcoming barriers imposed by the protein structure (*22*). A considerable number of O_2 molecules cannot overcome these barriers inside the protein matrix or the border between the protein and the solvent and return and rebind to heme iron atoms. Such a reaction is referred to as geminate recombination (GR). For those HbA subunits from which O_2 molecules succeed in escaping into the surrounding medium, rebinding is a bimolecular reaction (BR). Besides the oxygenation studies, the hemoglobin reactions with other small ligands (i.e., CO and NO) were also extensively studied (see, for example, refs *23−25*), in particular for comparison with myoglobin (*26*, *27*).

In a related approach to Gibson's work (*5*), the flash photolysis technique was extensively used in kinetic studies of the oxygenated hemoproteins (*5−21*). The earlier studies (*5−10*) dealt with bimolecular O_2 rebinding within microsecond and longer time ranges. The laser nanosecond flash photolysis technique has helped to identify a 50−100 ns component in the GR kinetics (*11−14*). Picosecond photoexcitation has provided a basis for GR investigation within the time range from several picoseconds up to 1.5 ns (*15*, *16*, *19*). The fast component (200 ps) of geminate recombination was detected for the first time in the work of Chernoff et al. (*15*). The complex biexponential geminate

[*] To whom correspondence should be addressed. Telephone: +375 172841620. Fax: +375 172840030. E-mail: bmd@imaph.bas-net.by.

[‡] Institute of Molecular and Atomic Physics.

[§] Institute of Physical Chemistry.

[1] Abbreviations: HbA, human hemoglobin; O_2, molecular oxygen; GR, geminate recombination; BR, bimolecular recombination.

recombination ($\tau_1 = 0.19$ ns and $\tau_2 = 1.6$ ns) with an offset component has been previously found (*16*, *19*). A considerable optical delay between exciting and probing pulses made it possible to study GR over the time range 1−95 ns (*17*).

The main objective of the work is to determine the complete oxygenation kinetics of R-state HbA from several picoseconds to several milliseconds using kinetic laser spectroscopy methods. This would enable us (i) to describe kinetically the O_2 motion in the interior of the protein, (ii) to estimate the efficiency of O_2 escape from the protein, and (iii) to measure the bimolecular rate constants of O_2 association with hemoglobin. It should be pointed out that the results of our studies of the bimolecular oxygenation reaction of native HbA and its isolated chains have been published recently (*10*). In the present paper, we shall analyze bimolecular oxygenation in the context of its relation with geminate oxygenation. These measurements will help us to find individual kinetic parameters of GR, which are yet unknown, for the α- and β-subunits within the tetramer.

MATERIALS AND METHODS

Oxyhemoglobin was isolated from fresh donor blood by the method described elsewhere (*28*). Oxyhemoglobin was separated into the α- and β-subunits by treating the protein (5×10^{-4} M) with a 10-fold excess of *p*-chlormercuribenzoate (PMB) in 0.02 M potassium phosphate buffer at pH 6.7 (*29*). The isolated α- and β-subunits were obtained by ion exchange chromatography on CM cellulose of PMB-treated oxyhemoglobin at pH ranging from 6.0 to 8.5 at the ionic strength from 0.01 to 0.02 M in potassium phosphate buffer at $+4$ °C (*29*).

The HbA concentrations are 100 and 400 μM on a per heme basis. At such concentrations, the dissociation of the tetrameric protein into dimers can be neglected.
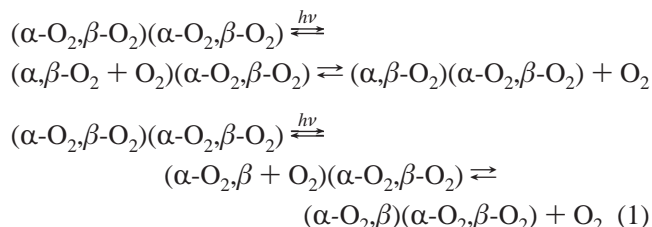
Picosecond and subnanosecond experiments are performed using a homemade pump−probe transient absorption spectrometer described in ref *30*. The samples are excited with the second harmonic (532 nm) of a YAG:Nd^{3+} solid-state master laser, while radiation of an optical parametric oscillator is used as a probing beam tunable over the entire visible region (380−1000 nm). An intracavity negative-feedback electrooptical system in combination with intracavity pulse selection provides sufficiently high stability of laser intensity (intensity scatter < 5%) and gives sufficiently high sensitivity and accuracy of the spectrometer (1×10^{-3} OD units). An optical delay line used in picosecond and subnanosecond experiments allows us to carry out transient absorption measurements on a time scale up to 3.2 ns. Delay line control, registration of laser beam intensities, data acquisition, and processing are performed with standard PC and CAMAC equipment. The time resolution of the above setup is approximately 20−25 ps as limited by the width of the probe and pump pulses.

A computer-controlled nanosecond spectrophotometer (*31*) used in laser flash spectroscopy studies is based on a nitrogen laser (PL 2300, PTI) serving both as a source of excitation and as a pump for a dye laser generating the monitoring light. Typical parameters of the nitrogen laser are as follows: the emission wavelength of 337 nm, the repetition rate up to 10 Hz, the pulse width ≤ 1 ns, and the pulse energy of approxi-

mately 1 mJ. The radiation of the nitrogen laser is divided into two beams by the splitter with a variable beam intensity ratio. Before being focused on the sample, the excitation beam is adequately delayed in a fixed optical delay line. The second beam pumps the dye laser. Tunable radiation produced by the dye laser enters a variable multipass optical delay line after collimation by a telescope. When the optical delay line is adjusted to get the longest optical path on a 2.5 m long guide rail, the monitoring pulse enters the sample 95 ns after excitation. In the present study, transient absorption kinetic curves are registered in the spectral region 430−440 nm. The time resolution of this setup is ∼1 ns.

Kinetic parameters for bimolecular oxygenation are measured using another nanosecond laser spectrometer (*10*). The second harmonic (532 nm) of an Nd:YAG laser serves as an exciting light pulse: the pulse duration is ∼20 ns, and the pulse energy ranges from 1.5 to 6.0 mJ. A halogen lamp, KGM12-100 (Brest Lamp Plant, Belarus), fed by a stabilized power supply is used as a probing light source. Lamp radiation is focused with a condenser on the sample. After passing the sample, the radiation enters a detecting monochromator equipped with a FEU-84 photomultiplier as a light detector, time resolution being ∼850 ns. Transient absorption measurements are performed in the spectral region 430−435 nm. The signals measured by the photodetector are digitized and visualized by a digital oscilloscope BORDO110 (Universal Enterprise "UNITECHPROM at the Belarusian State University", Minsk). The sensitivity of the detection system allows us to measure photoinduced absorption changes up to 1×10^{-5} absorbance unit.
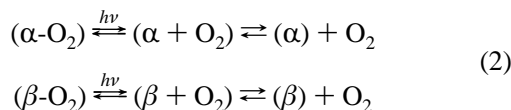
The kinetics of photoinduced HbA reoxygenation is studied under conditions when a small amount (no more than 1%) of O_2 is released from fully saturated HbA. Bearing in mind the contribution from geminate recombination, we assume that the primary photodissociation level does not exceed 10% (*19*). Such the photoexcitation level is used to ensure the experimental conditions when statistically each hemoglobin molecule loses only one molecule of oxygen and the tetrameric protein remains in the R-state (*32*). In fact, in experiment either of two sequences of events can be realized for an individual HbA molecule:

$$(\alpha\text{-}O_2,\beta\text{-}O_2)(\alpha\text{-}O_2,\beta\text{-}O_2) \overset{h\nu}{\rightleftharpoons}$$
$$(\alpha,\beta\text{-}O_2 + O_2)(\alpha\text{-}O_2,\beta\text{-}O_2) \rightleftharpoons (\alpha,\beta\text{-}O_2)(\alpha\text{-}O_2,\beta\text{-}O_2) + O_2$$

$$(\alpha\text{-}O_2,\beta\text{-}O_2)(\alpha\text{-}O_2,\beta\text{-}O_2) \overset{h\nu}{\rightleftharpoons}$$
$$(\alpha\text{-}O_2,\beta + O_2)(\alpha\text{-}O_2,\beta\text{-}O_2) \rightleftharpoons$$
$$(\alpha\text{-}O_2,\beta)(\alpha\text{-}O_2,\beta\text{-}O_2) + O_2 \quad (1)$$

Here $(\alpha\text{-}O_2,\beta\text{-}O_2)(\alpha\text{-}O_2,\beta\text{-}O_2)$ denotes oxyhemoglobin. In scheme 1, the oxygenated subunits are shown together with O_2; $(\alpha,\beta\text{-}O_2 + O_2)$ and $(\alpha\text{-}O_2,\beta + O_2)$ are monooxygenated HbA dimers. In this case, the photodissociated O_2 molecule still remains within the protein matrix. The right-hand terms in scheme 1 represent the case with free O_2 motion in the solution.

Additionally, the isolated α- and β-chains modified by *p*-chloromercuribenzoate (the α^{PMB}- and β^{PMB}-chains of HbA) are also studied. The choice of the modified α^{PMB}-,β^{PMB}-chains of HbA is not accidental. It is dictated by some

difficulties in obtaining the monomeric β^{SH}, since the protein consists of a dimer−tetramer mixture over a broad concentration range and experimental studies at 0.1 μM concentration, at which β^{SH} is mainly monomeric, are rather complicated. As for the β^{PMB}-chains, monomeric β^{PMB} can be obtained when solutions of this protein are at a higher concentration of 1 μM in heme. At heme concentration of 10 μM, α-chains are mainly monomeric. It is noteworthy that for the α^{PMB}- and α^{SH}-chains, the bimolecular association rate constants as well as the apparent quantum yields of photodissociation, γ, coincide (*16*). It has been shown (*16*) that within the time range from several picoseconds up to 1.5 ns these monomeric proteins have the close geminate recombinations. As for the monomeric β^{PMB}- and β^{SH}-chains, they also possess the same bimolecular association rate constants (*16, 33*). In this work, we measure kinetic parameters for the isolated α^{PMB}- and β^{PMB}-chains at concentrations 100, 10, and 2 μM. In our experiments, the following sequences of events are accomplished:

$$(\alpha\text{-}O_2) \overset{h\nu}{\rightleftharpoons} (\alpha + O_2) \rightleftharpoons (\alpha) + O_2$$
$$(\beta\text{-}O_2) \overset{h\nu}{\rightleftharpoons} (\beta + O_2) \rightleftharpoons (\beta) + O_2 \tag{2}$$

Notation used here corresponds to that of scheme 1.

Transient absorption decays are analyzed with a standard least-squares technique using a homemade software for PC. The deconvolution procedure is applied to correct the measured kinetics for the effect of instrumental response. The quality of fitting is determined by examining the Student coefficients for fitted function parameters and also by visual examination of residues. The bimolecular association rate constant k is calculated using the formula:

$$k = \frac{1}{\tau[O_2]} \tag{3}$$

where τ is the time of deoxygenated subunit binding to O_2. The time is derived from the experimental curve for photoinduced absorption change. $[O_2]$ is a concentration of molecular oxygen dissolved in the buffer. The measurements are made at 20 °C.

The primary quantum yield of photodissociation, γ_0, representing the ratio of the number of dissociated O_2 molecules to that of absorbed light quanta is determined as

$$\gamma_0 = \frac{\Delta A V}{\Delta \epsilon l \delta N} \tag{4}$$

where ΔA is the maximal change in the optical density of an oxyhemoglobin sample after photodissociation at the initial time moment, $\Delta \epsilon$ is the difference in the absorption coefficients for deoxygenated and oxygenated hemoglobin at the wavelength of observation, l is the optical path, δ is the fraction of absorbed light, and N is the number of photons striking upon a working volume V. The primary quantum yield of photodissociation is established (*16, 19*) to be the same ($\gamma_0 = 0.23 \pm 0.03$) both for the isolated HbA chains and for the tetramer. It should be emphasized that a very similar value, $\gamma_0 = 0.28 \pm 0.06$, was obtained for oxymyoglobin (*34*). Following the oxygenation recovery, the number of deoxygenated binding centers produced after photodissociation decreases. The ratio of the number of deoxygenated
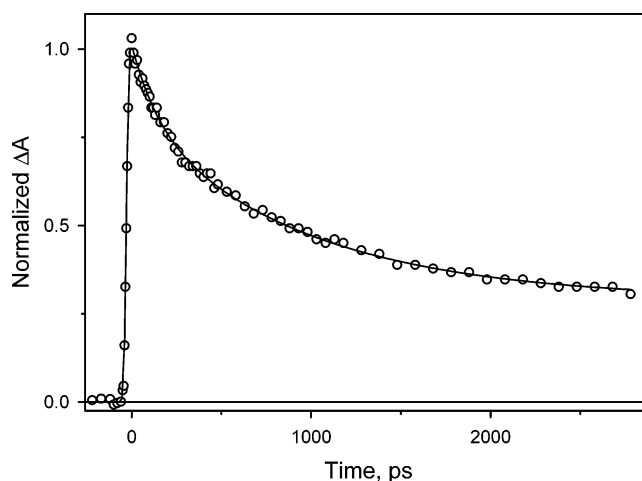

FIGURE 1: Normalized transient absorption decay corresponding to the recombination kinetics of O_2 with R-state HbA over the 0−3000 ps time range. Excitation wavelength, $\lambda_{exc} = 532$ nm; detection wavelength, $\lambda_{det} = 435$ nm. Conditions were 50 mM K_2HPO$_4$ buffer, pH 7.4, at 20 °C. HbA concentration = 100 μM in heme. The circles stand for our experimental data, and the solid line represents data fit by dual exponential plus constant. The observed maximal change in the optical density of the sample was 0.1 OD.

binding centers to that of absorbed light quanta will define an apparent quantum yield of dissociation. It is obvious that this ratio will be a function of time elapsed after the dissociation event and its value will be always smaller than γ_0. After GR is completed, the apparent quantum yield of photodissociation γ is properly responsible for the number of O_2 molecules that escape from the protein, and the ratio γ/γ_0 represents the efficiency of O_2 escape from the protein matrix. The apparent quantum yield γ is determined using a relative method previously discussed (*10*). HbA in 50 mM K_2HPO$_4$, pH 7.4, buffer is used as a reference standard, for which $\gamma = 0.026 \pm 0.003$ was obtained.

RESULTS

Time courses for triliganded R-state HbA oxygenation are shown in Figures 1, 2 (curve a), and 3 (curve a). Data analysis shows that the normalized oxygenation kinetics of triliganded R-state HbA in picosecond (0−3000 ps) and nanosecond (0−95 ns) time ranges can be modeled by the following equations:

$$\Delta A_{norm}^{ps} = a_1^{ps} \exp(-t/\tau_1^{ps}) + a_2^{ps} \exp(-t/\tau_2^{ps}) + a_{const}^{ps} \tag{5}$$

$$\Delta A_{norm}^{ns} = a_1^{ns} \exp(-t/\tau_1^{ns}) + a_2^{ns} \exp(-t/\tau_2^{ns}) + a_{const}^{ns} \tag{6}$$

where the superscripts "ps" and "ns" correspond to experimental data obtained for the picosecond (0−3000 ps) and nanosecond (0−95 ns) time ranges, respectively; ΔA_{norm} is a normalized change in optical density of the sample (Figures 1 and 2 (curve a)), a_i and τ_i ($i = 1,2$) are amplitudes and decay times of kinetic components, respectively, a_{const} is a constant component (offset). Table 1 lists the results for the kinetics approximated by eqs 5 and 6. Comparison of the results for the considered picosecond and nanosecond time ranges demonstrates that a common component with the decay time τ_2^{ps} (τ_1^{ns}) is present in the GR kinetics of triliganded R-state HbA for both time ranges. For this

Table 1: Kinetic Parameters for Oxygen Binding to R-State HbA and to the Isolated α- and β-Chains over the 0−3000 ps and 0−95 ns Time Ranges[a]

protein	time range (ps)	buffer	C (μM)[b]	τ_1^{ps} (ns)	τ_2^{ps} (ns)	a_1^{ps} (%)	a_2^{ps} (%)	a_{const}^{ps} (%)
HbA	0−3000	50 mM K_2HPO_4, pH 7.4	100	0.14 ± 0.02	0.98 ± 0.12	25 ± 3	49 ± 2	26 ± 3

protein	time range (ns)	buffer	C (μM)[b]	τ_1^{ns} (ns)	τ_2^{ns} (ns)	a_1^{ns} (%)	a_2^{ns} (%)	a_{const}^{ns} (%)
HbA	0−95	50 mM K_2HPO_4, pH 7.4	400	1.5 ± 0.2	29 ± 2	60 ± 3	25 ± 1	15 ± 2
α^{PMB}	0−95	50 mM K_2HPO_4, pH 7.4	50	1.3 ± 0.2	42 ± 4	48 ± 2	27 ± 2	26 ± 2
β^{PMB}	0−95	50 mM K_2HPO_4, pH 7.4	100	1.3 ± 0.2	54 ± 4	47 ± 2	33 ± 2	21 ± 2

[a] For kinetic parameters for the 0−3000 ps time range, the uncertainties are presented as 95% confidence intervals, while for the 0−95 ns time range, they are presented as standard errors. [b] Heme concentration.

component, we shall use the value of τ_2^{ps} obtained from the picosecond studies because the value of τ_1^{ns} received with lower time-resolution and signal-to-noise ratio. By convention, let us call the common component the 1 ns component. As a result, the constant component with the amplitude a_{const}^{ps} is defined as a sum of the longest nanosecond component with the decay time τ_2^{ns} and the contribution from bimolecular reactions. The constant component with the amplitude a_{const}^{ns} obtained from the nanosecond studies represents BR. Thus, a normalized kinetics of monomolecular geminate oxygenation of triliganded R-state HbA can be described by function of three exponentials and a constant component, which corresponds to more prolonged bimolecular nongeminate processes:

$$\Delta A_{norm} = \sum_{i=1}^{3} a_i \exp(-t/\tau_i) + a_4 \quad (7)$$

Equations 8−11 define amplitudes (a_i) of the components observable in the complete kinetics of the tetramer reaction:

$$a_1 = a_1^{ps} \quad (8)$$

$$a_2 = a_2^{ps} \quad (9)$$

$$a_3 = a_{const}^{ps} \frac{a_2^{ns}}{a_2^{ns} + a_{const}^{ns}} \quad (10)$$

$$a_4 = a_{const}^{ps} \frac{a_{const}^{ns}}{a_2^{ns} + a_{const}^{ns}} \quad (11)$$

Here a_1, a_2, and a_3 are the amplitudes of 0.14, 1, and 29 ns components of geminate recombination of R-state HbA, respectively, and a_4 is the amplitude of bimolecular oxygenation reactions. In tetrameric native HbA, a_4 relates to the efficiency of ligand escape from the protein into the environmental medium. Substitution of the experimental kinetic parameters (Table 1) into eqs 8−11 gives the amplitudes of the components to be $a_1 = 0.255 \pm 0.012$, $a_2 = 0.490 \pm 0.010$, $a_3 = 0.160 \pm 0.012$, and $a_4 = 0.096 \pm 0.014$. As it is mentioned in Materials and Methods, after GR is completed, the ratio γ/γ_0 determines the efficiency of O_2 escape from the protein matrix. Thus, based on the calculated value of a_4, the apparent quantum yield of photodissociation γ and the primary quantum yield γ_0 differ by an order of magnitude as
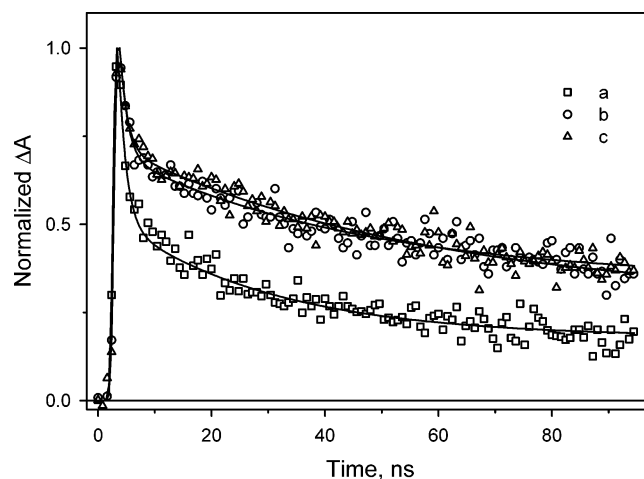
$$a_4 = \gamma/\gamma_0 \quad (12)$$

FIGURE 2: Normalized transient absorption decays corresponding to the recombination kinetics of O_2 with R-state HbA and with the isolated chains over the 0−95 ns time range. Excitation wavelength, $\lambda_{exc} = 337$ nm; detection wavelength, $\lambda_{det} = 430$ nm. Conditions were 50 mM K_2HPO_4 buffer, pH 7.4, at 20 °C. Heme concentration, [HbA] = 400 μM (a); [α^{PMB}] = 50 μM (b); [β^{PMB}] = 100 μM (c). Symbols correspond to our experimental data, and the solid lines show data fit with biexponential function plus constant. The number of experimental data points on the figures is reduced with a factor of 4 for clarity. The observed maximal changes in the optical density of the samples were 0.3 OD.

Having this in mind, let us consider the agreement of the experimental values of γ_0 and γ measured with help of different experimental setups for various time ranges. In refs *16* and *19*, the values of the primary quantum yield, $\gamma_0 = 0.23 \pm 0.03$, and the apparent quantum yield of photodissociation, $\gamma = 0.026 \pm 0.003$, have been determined independently of each other. Using eq 12, one can take the value of $\gamma_0 = 0.23 \pm 0.03$ and obtain a value of $\gamma = 0.022 \pm 0.004$. Alternatively, for $\gamma = 0.026 \pm 0.003$ eq 12 yields $\gamma_0 = 0.27 \pm 0.05$. This shows a good agreement between the measured values of the quantum yields γ and γ_0.

Time courses for oxygenation of the isolated α^{PMB}- and β^{PMB}-chains are shown in Figures 2 (curves b and c) and 3 (curves b and c). The normalized oxygenation kinetics of the isolated chains in the nanosecond (0−95 ns) time range can be modeled by eq 6. The results of fitting are summarized in Table 1. One can see (Table 1) that there are differences in the kinetics of the isolated α^{PMB}- and β^{PMB}-chains and HbA (Figure 2). HbA is characterized by the increased amplitude $a_1^{ns} = 60\% \pm 3\%$ of the 1 ns component and by the smaller amplitude $a_{const}^{ns} = 15\% \pm 2\%$ of the constant component. The apparent increase of the value a_1^{ns} of the 1 ns component can be caused by the 0.14 ns component superimposed on the 1 ns component. Additionally, tet-

Table 2: Kinetic Parameters for Oxygen Binding to R-State HbA and to the Isolated α- and β-Chains over the 0−2000 μs Time Range[a]

protein	buffer	C (μM)[b]	k_β (μM·s)$^{-1}$	k_α (μM·s)$^{-1}$	a_β (%)	a_α (%)	γ_β	γ_α	γ
HbA	50 mM K$_2$HPO$_4$, pH 7.4	100	52 ± 4	18.8 ± 1.3	78 ± 3	22 ± 3	0.041 ± 0.004	0.0114 ± 0.0012	0.026 ± 0.002
HbA	10 mM Tris HCl, pH 7.4	100	62.9 ± 1.6	27.2 ± 1.3	79 ± 2	21 ± 2	0.036 ± 0.004	0.010 ± 0.001	0.023 ± 0.002

protein	buffer	C (μM)[b]	k (μM·s)$^{-1}$	γ
α^{PMB}	50 mM K$_2$HPO$_4$, pH 7.4	100	44 ± 2	0.056 ± 0.006
α^{PMB}	50 mM K$_2$HPO$_4$, pH 7.4	10	46 ± 2	
α^{PMB}	50 mM K$_2$HPO$_4$, pH 7.4	2	44 ± 2	
β^{PMB}	50 mM K$_2$HPO$_4$, pH 7.4	100	49 ± 1	0.068 ± 0.007
β^{PMB}	50 mM K$_2$HPO$_4$, pH 7.4	10	52 ± 2	
β^{PMB}	50 mM K$_2$HPO$_4$, pH 7.4	2	51 ± 1	

^{a} For kinetic parameters for the 0−2000 μs time range, the uncertainties are presented as 95% confidence intervals. ^{b} Heme concentration.
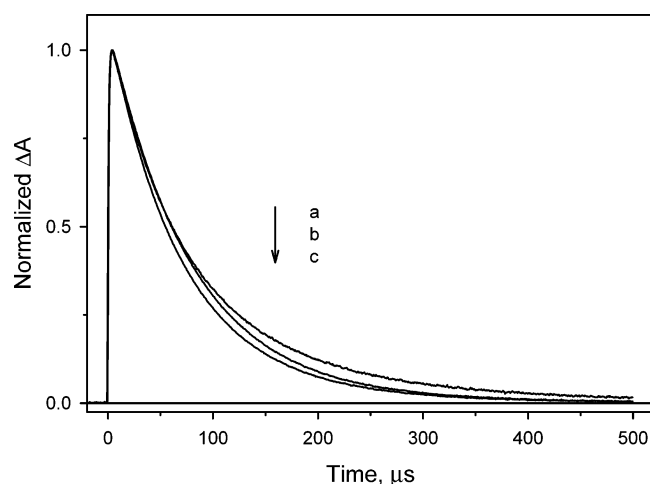

FIGURE 3: Normalized transient absorption decays corresponding to the recombination kinetics of O$_2$ with R-state HbA and with its isolated chains over the 0−500 μs time range. Excitation wavelength, λ_{exc} = 532 nm; detection wavelength, λ_{det} = 430 nm. Conditions were 50 mM K$_2$HPO$_4$ buffer, pH 7.4, at 20 °C. Heme concentration, [HbA] = 100 μM (a); [α^{PMB}] = 100 μM (b); [β^{PMB}] = 100 μM (c). The observed maximal changes in the optical density of the samples were 0.01 OD (HbA), 0.02 OD (α^{PMB}), and 0.025 (β^{PMB}).

rameric HbA demonstrates a shorter value (τ_2^{ns} = 29 ± 2 ns) of the decay time for the slowest GR component in comparison with values 42 ± 4 and 54 ± 4 ns for the α^{PMB}- and β^{PMB}-chains, respectively.

Results of the bimolecular oxygenation studies are presented in Figure 3. The normalized oxygenation kinetics of triliganded R-state HbA over the microsecond (0−2000 μs) time range is fitted with a biexponential function:

$$\Delta A_{norm}^{\mu s} = a_\beta \exp(-t/\tau_\beta) + a_\alpha \exp(-t/\tau_\alpha) \qquad (13)$$

where ΔA_{norm} is a normalized change in optical density of the sample (Figure 3, curve a) and a_α, a_β, τ_α, and τ_β are amplitudes and decay times of exponentials. Table 2 lists the bimolecular recombination rate constants k derived from the decay times τ_α and τ_β using eq 3, together with the amplitudes of the components of bimolecular processes. On the basis of the considerations described in refs *8* and *10*,

these two bimolecular processes are assigned to bimolecular oxygenation of the β- and α-subunits within triliganded tetrameric R-state HbA. The amplitude ratio a_β/a_α and the value $\gamma = 0.026 \pm 0.003$ of the apparent quantum yield of R-state HbA photodissociation indicate that the apparent quantum yields of photodissociation of the β- and α-subunits within completely oxygenated native R-state HbA differ from each other by a factor of 3.6 and are equal to 0.041 ± 0.004 and 0.0114 ± 0.0012, respectively (Table 2).

The bimolecular oxygenation kinetics of the isolated α^{PMB}- and β^{PMB}-chains (Figure 3) are approximated by monoexponential functions. Our data show that the change in the heme concentration of the α^{PMB}-chains from 100 to 2 μM does not affect, within the experimental accuracy, the rate constant for O$_2$ association with the α^{PMB}- chain, $k_\alpha = 44 \pm 2$ (μM·s)$^{-1}$ (Table 2, Figure 3, curve b). As the protein concentration is varied, the invariance of k_α values is attributed to the essentially monomeric form of the α^{PMB}-chain in the considered concentration range. In the case of the β^{PMB}-chains, the same effect is obvious. As the heme concentration is decreased from 100 to 2 μM, we find that the association rate constant is essentially unaltered $k_\beta = 49 \pm 1$ (μM·s)$^{-1}$ and $k_\beta = 51 \pm 1$ (μM·s)$^{-1}$, respectively (Table 2, Figure 3, curve c). On the basis of the experimental results for the monomeric α^{PMB}- and β^{PMB}-chains, it can be concluded that O$_2$ rebinding with the β^{PMB}-chains proceeds 1.2 times faster than oxygenation of α^{PMB}, and the efficiency of the ligand escape from the β^{PMB}-chains into the surrounding medium is 1.2 times greater than the one from the α^{PMB}-chains.

DISCUSSION

As it is shown in Results, several different decay components are detected in the time courses for triliganded R-state HbA oxygenation. There is a reason to believe that in the present experiment (i) the origin of all observed spectral changes is ligand rebinding and (ii) all possible GR stages should be seen. It should be specially pointed out that the largest difficulties are encountered in the analysis of the events during the first few picoseconds after photoexcitation of oxygenated HbA. Some authors reported two intermediates with lifetimes of ~300 fs and 2−3 ps (see, for example, ref

Table 3: Calculated Contributions ($w_{i\alpha}$ and $w_{i\beta}$) of the α- and β-Subunits to the ith Component of the Reaction between O_2 and Triliganded R-State HbA and Calculated Amplitudes ($a_{i\alpha}$ and $a_{i\beta}$) of the ith Component in the Reaction between O_2 and the α- and β-Subunits of Triliganded R-State HbA

$w_{1\alpha}$	$w_{2\alpha}$	$w_{3\alpha}$	$w_{4\alpha}$	$w_{1\beta}$	$w_{2\beta}$	$w_{3\beta}$	$w_{4\beta}$
0.85 ± 0.25	0.54 ± 0.10	0.00 ± 0.20	0.22 ± 0.01	0.15 ± 0.25	0.46 ± 0.10	1.00 ± 0.20	0.78 ± 0.01
$a_{1\alpha}$	$a_{2\alpha}$	$a_{3\alpha}$	$a_{4\alpha}$	$a_{1\beta}$	$a_{2\beta}$	$a_{3\beta}$	$a_{4\beta}$
0.43 ± 0.13	0.52 ± 0.10	0.00 ± 0.06	0.042 ± 0.006	0.08 ± 0.13	0.45 ± 0.10	0.32 ± 0.07	0.15 ± 0.02

35). It is, however, hardly possible to assign such fast components to any possible geminate recombination process, so the ~300 fs and 2−3 ps decays mentioned seem to be caused by other reasons (heme cooling and excited-state absorption) (see, for example, refs *21* and *36*). Further, the photolysis extent (~10%) is insufficient to drive the R → T quaternary transition. Therefore, only tertiary relaxations can occur after photodissociation. Furthermore, both optical absorption (*15*) and resonance Raman experiments (*37*) have failed to reveal any spectral changes associated with the tertiary conformational changes in the 10 ps to 10 ns time range. In solution at room-temperature geminate recombination can occur over a temporal window extended from a few picoseconds up to several hundred nanoseconds. This time scale is faster than the time scales for large-amplitude tertiary relaxations (1 μs).

As mentioned above, in the experiment, one of two sequences of events (see scheme 1) can be realized with one individual HbA molecule. Consequently, after photodissociation in the hemoglobin solution, two reactions are simultaneously initiated: one reaction occurs with the participation of the α-subunits and the other with the participation of the β-subunits of triliganded R-state HbA. Hence, any determined amplitude a_i (eq 7) of the ith component of the reaction between O_2 and triliganded R-state HbA can be divided into two constituents:

$$a_{i\alpha} = 2w_{i\alpha}a_i, \quad i = \overline{1,4} \tag{14}$$

$$a_{i\beta} = 2w_{i\beta}a_i, \quad i = \overline{1,4} \tag{15}$$

Here $a_{i\alpha}$ and $a_{i\beta}$ are amplitudes of the ith component in the reaction between O_2 and the α- and β-subunits of HbA, respectively. $w_{i\alpha}$ and $w_{i\beta}$ are contributions of the α- and β-subunits to the ith component of the reaction between O_2 and HbA. These contributions satisfy the condition $w_{i\alpha} + w_{i\beta} = 1$. The condition for normalization of the amplitude sum is

$$\sum_{i=1}^{4} a_{i\alpha} = 1, \quad \sum_{i=1}^{4} a_{i\beta} = 1, \quad \sum_{i=1}^{4} a_i = 1 \tag{16}$$

Equation 16 is valid because there is a sufficient reason indicating that the primary quantum yields γ_0 of photodissociation for the HbA subunits are equal to the value $\gamma_0 = 0.23 \pm 0.03$, which has been found for oxygenated R-state HbA and its isolated subunits (*16*).

Now let us analyze all available information on the individual properties of the α- and β-subunits within HbA. As it can be seen from Table 2, the contribution of the α- and β-subunits to BR is equal to $w_{4\alpha} = a_\alpha = 0.22 \pm 0.03$ and $w_{4\beta} = a_\beta = 0.78 \pm 0.03$, respectively. The value of the

association rate constant $k_\alpha = 44 \pm 2$ $(\mu M \cdot s)^{-1}$ and a value of the apparent quantum yield of photodissociation $\gamma = 0.056 \pm 0.006$ for the isolated α^{PMB}-chain exceed corresponding values $k_\alpha = 18.8 \pm 1.3$ $(\mu M \cdot s)^{-1}$ and $\gamma = 0.0114 \pm 0.0012$ obtained for the α-subunit within HbA. The smaller changes are seen in the kinetic parameters for the β-subunits. The apparent quantum yields of photodissociation differ less, 0.068 ± 0.007 and 0.041 ± 0.004 for the isolated β^{PMB}-chain and β-subunit within HbA, respectively. The association rate constant $k_\beta = 51 \pm 1$ $(\mu M \cdot s)^{-1}$ for the isolated β^{PMB}-chain coincides with $k_\beta = 52 \pm 4$ $(\mu M \cdot s)^{-1}$ for the β-subunit within HbA. As it can be seen, the considered kinetic parameters of bimolecular oxygenation of both the isolated β^{PMB}-chain and β-subunit within HbA molecule are relatively close to each other. As a result, we should expect that upon transformation of the β-subunit from the isolated state into the incorporated state (within R-state HbA), GR components are not principally affected, the amplitudes of the corresponding components are not altered significantly, and hence, their ratio undergoes no marked changes. But for the α^{PMB}-chains, a different picture of GR can be suggested: the longest GR component of R-state HbA is negligible or absent for the α-subunit within HbA. This assumption is supported by the results of cobalt−iron hybrid hemoglobin studies (*13*), which have shown the presence and the absence of the longest GR component of R-state HbA in the β- and α-subunits within HbA, respectively. Hence, $w_{3\alpha} = 0.0 \pm 0.2$ and $w_{3\beta} = 1.0 \pm 0.2$ can be used as the contributions of the α- and β-subunits to the longest (29 ns) GR component of R-state HbA.

Now the values $a_{i\alpha}$ and $a_{i\beta}$ (Table 3) can be found and overall oxygenation kinetics of the α- and β-subunits within triliganded R-state HbA can be presented by the following equations:
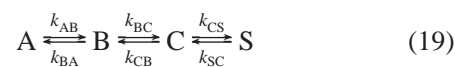
$$\Delta A^{\alpha}_{norm} = (0.43 \pm 0.13) \exp(-t/(0.14 \text{ ns})) + (0.52 \pm 0.10) \exp(-t/(1 \text{ ns})) + (0.00 \pm 0.06) \exp(-t/(29 \text{ ns})) + (0.042 \pm 0.006) \exp((-18.8 \, (\mu M \cdot s)^{-1})t[O_2]) \tag{17}$$

$$\Delta A^{\beta}_{norm} = (0.08 \pm 0.13) \exp(-t/(0.14 \text{ ns})) + (0.45 \pm 0.10) \exp(-t/(1 \text{ ns})) + (0.32 \pm 0.07) \exp(-t/(29 \text{ ns})) + (0.15 \pm 0.02) \exp((-52 \, (\mu M \cdot s)^{-1})t[O_2]) \tag{18}$$

where the superscripts "α" and "β" correspond to overall O_2 rebinding with the α- and β-subunits within triliganded R-state HbA, respectively, and ΔA_{norm} is a normalized change in optical density. As it follows from the calculated data (Table 3), the contribution of the α-subunit to the 0.14 ns component of geminate recombination of R-state HbA is predominant ($w_{1\alpha} = 0.85 \pm 0.25$). Accordingly,

the contribution of the β-subunit to the 0.14 ns component is not significant or is absent ($w_{1\beta} = 0.15 \pm 0.25$). Using the values of $w_{2\alpha}$ and $w_{2\beta}$, we may conclude that the 1 ns component of geminate recombination of R-state HbA is equally shared by both the α- and β-subunit. The origin of the remaining components is considered above. As shown in ref *16*, no 0.14 ns component of GR has been found for the isolated α- and β-chains in the 0–1500 ps time range. These results of the previous picosecond studies (*16*) are supported by the following data of the present studies. By multiplying the value 0.056 ± 0.006 (0.068 ± 0.007) of the apparent quantum yield γ for the isolated α^{PMB} (β^{PMB}) chain with the constant component $a_{const}^{ns} = 0.26 \pm 0.02$ (0.21 ± 0.02), we can obtain the value of the primary quantum yield $\gamma_0 = 0.22 \pm 0.03$ (0.32 ± 0.04). These calculated values are in a sufficiently good agreement with the measured primary quantum yield, $\gamma_0 = 0.23 \pm 0.03$, indicating the absence of the ~0.14 ns GR component for the isolated chains. Consequently, monomolecular geminate oxygenation of the isolated chains can be modeled as a sum of two exponentials and a constant (eq 6).

The detailed analysis of the oxygenation parameters of the subunits both in the isolated state and within HbA molecules reveals some interesting experimental features. As it has been shown, the isolated α^{PMB}- and β^{PMB}-chains display the ~1 ns GR component with amplitudes being approximately the same (~50%) for both isolated chains. Upon transition of the β-subunits from the isolated state into the packed state (within the tetramer), the oxygenation kinetic parameters are not change principally. Nevertheless, the decrease of the decay time τ_2^{ns} from 54 ± 4 ns (isolated state) to 29 ± 2 ns (R-state HbA) occurs. This change is accompanied by the decrease in the apparent quantum yield γ from 0.068 ± 0.007 to 0.041 ± 0.004. These facts can indicate β-subunit conformational changes, which cause the appreciable decrease of the decay time of geminate recombination and the probability of O_2 escape from the protein. In contrast to the β-subunits, the properties of the α-subunits proved to be more sensitive to whether the subunits are in the isolated state or incorporated into the tetramer. After the α-subunits are packed into the tetramer, a new GR component appears with the decay time 0.14 ± 0.02 ns. However the 1 ns component is still observed with practically unchanged contribution (~50%). The intriguing conservation of the decay time (1 ns) and the amplitude (~50%) prompts us to discuss a possible formal kinetic model that can describe and explain such behavior of the parameters. There are many possible schemes, including parallel and more sophisticated mixed schemes (see, for example, refs *38* and *39*). At the present time, there is no a priori basis for selecting the best scheme. Within the framework of wells models, any oxygen binding scheme that reduces to two exponential decays can represent separately the kinetics both for the isolated chains and for the subunits incorporated into the tetramer. At least four wells are required to fit two-exponential geminate recombination time courses. Let us begin with an analysis of O_2 binding within the framework of a simple phenomenological sequential model

$$A \underset{k_{BA}}{\overset{k_{AB}}{\rightleftharpoons}} B \underset{k_{CB}}{\overset{k_{BC}}{\rightleftharpoons}} C \underset{k_{SC}}{\overset{k_{CS}}{\rightleftharpoons}} S \tag{19}$$

with a number of geminate intermediates with the single path for oxygen molecule leaving and entering the bulk protein. Most authors agree that at room-temperature ligand binding to protein can be described by this linear mechanism involving three consecutive reaction processes (*26, 38–40*). In scheme 19, the molecular oxygen must overcome several barriers. State A corresponds to the bound state containing the ligand covalently attached to the heme iron atom; state S corresponds to a state where a free ligand molecule is in the solvent phase. State B represents the initial geminate state following disruption of the iron–ligand bond; state C represents a state distinct from state B where the ligand is still embedded in the protein matrix but farther away from the iron atom. State C can be pictured as a pocket outside of the heme pocket from which the ligand escapes to the solvent.

To answer the question, if sequential model 19 can describe the abovementioned conservation of the decay time (1 ns) and the amplitude (~50%), the empirical kinetic parameters τ_1^{ns}, τ_2^{ns}, a_1^{ns}, and a_2^{ns} (eq 6) of the GR components of the isolated α^{PMB}-chain should be expressed in terms of rate constants of ligand movement between the states of scheme 19. The considered empirical parameters can be expressed through the rate constants by analytical solution of the following system of coupled differential equations (eq 20) for sequential model 19.
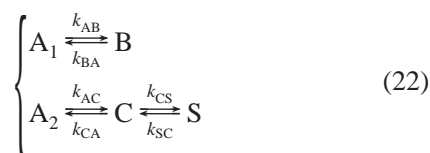
$$\begin{cases} \dfrac{d[A]}{dt} = k_{BA}[B] - k_{AB}[A] \\[2mm] \dfrac{d[B]}{dt} = k_{AB}[A] + k_{CB}[C] - (k_{BA} + k_{BC})[B] \\[2mm] \dfrac{d[C]}{dt} = k_{BC}[B] + k_{SC}[S] - (k_{CB} + k_{CS})[C] \\[2mm] \dfrac{d[S]}{dt} = k_{CS}[C] - k_{SC}[S] \end{cases} \tag{20}$$

Here [A], [B], [C], and [S] denote state concentrations. All states, except for state A, exhibit spectral properties of unliganded subunit; only when state A is formed or decayed is a spectral change observed. The system of coupled differential equations is simplified by omitting the rate of thermal dissociation, k_{AB}. This rate is negligible low compared with the photodissociation rate. The rate of ligand entry into protein from the solvent, k_{SC}, is also set to zero because of the negligible contribution that bimolecular recombination makes during the first 100 ns after photoradiation. The initial concentrations of states A, C, and S are set to 0, while that of state B is set equal to 1. This is an arbitrary initial condition. It reflects only our prior assertion that, after a few picoseconds of laser irradiation, the free ligand inside the distal pocket and pentacoordinate heme (the spectral features of this heme are similar to ones for the deoxy-protein) is already the photolysis product (state B) of six-coordinated heme (state A). Thus, solution of the differential equations with the accepted initial conditions allows us to write the required empirical parameters in terms of sequential model 19:

$$\begin{cases} \tau_1^{ns} = \dfrac{2}{k_{BA} + k_{BC} + k_{CB} + k_{CS} + \sqrt{p}} \\[2mm] \tau_2^{ns} = \dfrac{2}{k_{BA} + k_{BC} + k_{CB} + k_{CS} - \sqrt{p}} \\[2mm] a_1^{ns} = \dfrac{k_{BA}((k_{CB} + k_{CS})(k_{BA} + k_{BC} - k_{CB} - k_{CS} + \sqrt{p}) - 2k_{BC}k_{CB})}{2\sqrt{p}((k_{BA} + k_{BC})(k_{CB} + k_{CS}) - k_{BC}k_{CB})} \\[2mm] a_2^{ns} = \dfrac{k_{BA}((k_{CB} + k_{CS})(k_{CB} + k_{CS} - k_{BA} - k_{BC} + \sqrt{p}) + 2k_{BC}k_{CB})}{2\sqrt{p}((k_{BA} + k_{BC})(k_{CB} + k_{CS}) - k_{BC}k_{CB})} \\[2mm] p = (k_{BA} + k_{BC})^2 + (k_{CB} + k_{CS})^2 + 4k_{BC}k_{CB} - 2(k_{BA} + k_{BC})(k_{CB} + k_{CS}) \end{cases}$$
(21)

After the isolated α^{PMB}-chains are packed into the tetramer, a new GR component appears with the decay time 0.14 ± 0.02 ns. This means that rate constants of ligand movement between the states are changed. As can be shown from eq 21, it is very unlikely that, simultaneously, the decay time and the amplitude remain unchanged with rate constant variation. In another words, sequential model 19 is not appropriate to describe present experimental data of ligand rebinding with the α-subunits. As will be shown below, the following parallel model

$$\begin{cases} A_1 \underset{k_{BA}}{\overset{k_{AB}}{\rightleftarrows}} B \\[2mm] A_2 \underset{k_{CA}}{\overset{k_{AC}}{\rightleftarrows}} C \underset{k_{SC}}{\overset{k_{CS}}{\rightleftarrows}} S \end{cases}$$
(22)

can describe ligand rebinding within the isolated α^{PMB}-chain and can explain adequately the behavior of the empirical GR parameters (the decay times and the amplitudes) upon the α-subunit transition from the isolated state to the packed state. Recombination model 22 includes parallel reactions, which can occur in a single protein conformation. This assumes that ligand-bound states A_1 and A_2 should be considered as just the same state A, containing the ligand covalently attached to the heme iron atom. After ligand photodissociation within the isolated α^{PMB}-chain, the system goes from state A to state B or to state C. State C represents a protein cavity from which the ligand may escape to the solvent. The ligand has no chance to escape from a protein cavity represented by state B. State S corresponds to movement of a free ligand molecule in the solvent phase. It is supposed that the internal globin space (including the heme pocket subunit space) can be divided into two parts with relatively high barrier for oxygen motion from one part to another. This internal globin space division means that immediately after photodissociation, heme pocket amino acid residues can determine the reaction paths. The experimentally observed rate constant of bimolecular oxygenation for the isolated α^{PMB}-chain is assigned to ligand rebinding from the solvent to the deoxygenated chain through intermediate state C. Upon the α-subunit transition from the isolated state to the packed state, the observed changes of the apparent quantum yield and the rate constant of bimolecular oxygenation are assumed to accompany the measured change of geminate recombination. Similar to the previous models, the rates of thermal dissociation, k_{AB} and k_{AC}, and the rate of ligand entry into protein from the solvent, k_{SC}, are omitted. Therefore the detected decay times and amplitudes of geminate recombination can be expressed through the rate constants for scheme 22. To comply with the observation of

the 1 ns GR component being not affected by the subunit packing, one needs to assign the 1 ns component of ligand movement in pathway

$$A_1 \underset{k_{BA}}{\longleftarrow} B$$
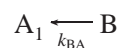
This channel does not lead to the solvent phase. Consequently, after tetramerization the pathway cannot be blocked by adjacent HbA subunits or changed by inclusion of internal cavities of adjacent subunits of R-state HbA molecule. Thereby, all O_2 that can reach the first cavity (state B) move never into the solvent but rebind from the protein in time $\sim$ 1 ns ($1/k_{BA}$) and have no chance to escape from the protein matrix. But being in the another cavity (state C), the O_2 molecule rebinds within the isolated α^{PMB}-chain in 42 ± 4 ns ($1/(k_{CS} + k_{CA})$) or has the chance to escape from the protein with the efficiency 0.24 ± 0.04. Upon subunit packing, this second channel of O_2 motion displays some substantial changes. As a result, we can see the disappearance of the 42 ± 4 ns GR component, the appearance of a new 0.14 ns GR component for the α-subunit within R-state HbA, and the decreased efficiency of O_2 escape from the protein matrix. These can be associated with two possible effects. The first effect is a decrease of the internal volume for dissociated ligand by changing positions of amino acid residues, which determine ligand path trajectories $A_2 \rightleftarrows C \rightleftarrows S$. The second one is "plugging" pathways $A_2 \rightleftarrows C \rightleftarrows S$ and opening new alternative pathways $A_2 \rightleftarrows D \rightleftarrows S$. Here state D represents a geminate state differing from state C in amino acid residues, which determine ligand path trajectories. The equal values ($\sim 50\%$) of probabilities of states B and C (D) state populations after photodissociation can be due to randomly distributed directions of initial ligand motion on the unit hemisphere on the distal side of the heme. Such distribution of probabilities leads to an assumption about two channels of O_2 motion in the opposite directions relative to the heme iron atom. This suggestion is in accordance with the results of molecular dynamics simulation (41). It has been shown that trajectories can involve so-called classic "short path" (motion very nearly parallel to the heme plane of the α chain, out of the heme pocket between His(E7) and Val(E11)), and motion in the quite opposite direction of pyrrole I (41). Parallel model 22 can also describe ligand rebinding both in the isolated β^{PMB}-chain and in the triliganded R-state HbA with one deoxygenated β-subunit. Obviously, both channels of ligand movement within the isolated β^{PMB}-chain do not undergo marked modifications upon the β-subunit transition from the isolated state to the packed state.

Now we do not discuss in detail a concrete division of a globin space, including the heme pocket cavity, possible concrete oxygen trajectories, and amino acids residues responsible for the observed kinetics. Investigations of mutagenesis effect on geminate and bimolecular O_2 rebinding to mutants at different positions is required to map pathways for ligand movement in to and out of the considered proteins. It is possible that proposed parallel model 22 is oversimplified for the description of ligand rebinding with the α- and β-subunits. Perhaps, the ligand escapes through the interior of protein by multiple transiently formed hydrophobic channels that eventually lead to the solvent phase. The histidine gate is likely to be not the primary pathway for

ligand movement in to and out of protein. This discussion will be given elsewhere.

CONCLUSIONS

We have found a kinetic description of dioxygen rebinding with triliganded R-state HbA and presented the parameters that describe oxygenation of the α- and β-subunits within the tetramer. The α-chain changes its properties markedly upon transformation from the isolated state into the incorporated state (within R-state HbA): the appearance of the 0.14 ns GR component and the disappearance of the slow (42 ns) GR component are observed. In contrast to the α-subunit, the β-subunit maintains its properties largely upon transformation from the isolated state into the incorporated state. The experimental data presented in the study indicate that the β-subunit of fully oxygenated HbA shows less efficient geminate recombination and thus indicate higher probability of O_2 escape into the surrounding medium. The distal pocket of the β-subunit within R-state HbA is more accessible for oxygen molecules dissolved in the surrounding medium. Additional experiments would be required to assign the above-mentioned protein cavities to concrete protein regions. This elucidation is of immediate interest to understanding of protein structure−dynamics relation.

REFERENCES

1. Perutz, M. F., Wilkinson, A. J., Paoli, M., and Dodson, G. G. (1998) The stereochemical mechanism of the cooperative effects in hemoglobin revisited, *Annu. Rev. Biophys. Biomol. Struct. 27*, 1−34.
2. Antonini, E., and Brunori, M. (1971) *Hemoglobin and Myoglobin in their Reaction with Ligands*, North-Holland, Amsterdam.
3. Parkhust, L. J. (1979) Hemoglobin and myoglobin ligand kinetics, *Annu. Rev. Phys. Chem. 30*, 503−546.
4. Ho, Ch. (1992) Proton nuclear magnetic resonance studies on hemoglobin: cooperative interactions and partially ligated intermediates, *Adv. Protein Chem. 43*, 153−312.
5. Gibson, Q. H. (1959) The photochemical formation of a quickly reacting form of haemoglobin, *Biochem. J. 71*, 293−303.
6. Mathews, A. J., Rohlfs, R. J., Olson, J. S., Tame, J., Renaud, J.-P., and Nagai, K. (1989) The effects of E7 and E11 mutation on the kinetics of ligand binding to R state human hemoglobin, *J. Biol. Chem. 264*, 16573−16583.
7. Unzai, S., Eich, R., Shibayama, N., Olson, J. S., and Morimoto, H. (1998) Rate constant for O_2 and CO binding to the α and β subunits within the R and T states of human hemoglobin, *J. Biol. Chem. 273*, 23150−23159.
8. Philo, J. S., and Lary, J. W. (1990) Kinetic investigations of the quaternary enhancement effect and α/β differences in binding the last oxygen to hemoglobin tetramers and dimers, *J. Biol. Chem. 265*, 139−143.
9. Dzhagarov, B. M., and Kruk, N. N. (1996) Bohr alkaline effect: regulation of the binding of O_2 to triliganded haemoglobin Hb-$(O_2)_3$, *Biophysics (Engl. Transl.) 41*, 607−612.
10. Lepeshkevich, S. V., Konovalova, N. V., and Dzhagarov, B. M. (2003) Laser kinetic studies of bimolecular oxygenation reaction of α and β subunits within the R state of human hemoglobin, *Biokhimiya (Moscow) 68*, 676−685.
11. Alpert, B., Banerjee, R., and Lindqvist, L. (1974) The kinetics of conformational changes in hemoglobin, studied by laser photolysis, *Proc. Natl. Acad. Sci. U.S.A. 71*, 558−562.
12. Duddell, D. A., Morris, R. J., Muttucumaru, N. J., and Richards, J. T. (1980) The dependence of the quantum yield of ligand

13. Morris, R. J., Gibson, Q. H., Ikeda-Saito, M., and Yonetani, T. (1984) Geminate combination of oxygen with iron−cobalt hybrid hemoglobins, *J. Biol. Chem. 259*, 6701−6703.
14. Olson, J. S., Rohlfs, R. J., and Gibson, Q. H. (1987) Ligand recombination to the α and β subunits of human hemoglobin, *J. Biol. Chem. 262*, 12930−12938.
15. Chernoff, D. A., Hochstrasser, R. M., and Steele, A. W. (1980) Geminate recombination of O_2 and hemoglobin, *Proc. Natl. Acad. Sci. U.S.A. 77*, 5606−5610.
16. Dzhagarov, B. M., Galievsky, V. A., Kruk, N. N., and Yakutovich, M. D. (1999) Photodissociation of oxygenated forms of the native hemoglobin HbA and its isolated α- and β-subunits and kinetics of molecular oxygen rebinding, *Dokl. Biophys. (Transl. of Dokl. Akad. Nauk) 366*, 38−41.
17. Sazanovich, I. V., Galievsky, V. A., Karpiuk, J., Petrov, E. P., Waluk, J., and Dzhagarov, B. M. (2001) Kinetic description of dioxygen binding to human hemoglobin on the 1−100 ns time scale, *Proc. SPIE 4749*, 355−359 (Chikishev, A. Y., Orlovich, V. A., Rubinov, A. N., and Zheltikov A. M., Eds.).
18. Hochstrasser, R. M., and Johnson, C. K. (1988) Biological processes studied by ultrafast laser techniques, in *Ultrashort Laser Pulses and Applications* (Kaiser, W., Ed.) pp 357−380, Springer-Verlag, Berlin.
19. Dzhagarov, B. M., Kruk, N. N., Tikhomirov, S. A., and Galievsky, V. A. (1996) Hemoglobin oxygenation dynamics on picosecond time scale, in *Ultrafast Processes in Spectroscopy IX* (Svelto, O., De Silvestro, S., and Denardo, G., Eds.) pp 497−502, Plenum Publishing Corporation, New York.
20. Dzhagarov, B. M., Kruk, N. N., Tikhomirov, S. A., and Stepuro, I. I. (1995) Laser kinetic spectroscopy studies of the reaction of human hemoglobin with molecular oxygen, *Proc. SPIE 2370*, pp 232−241 (Apanasevich, P. A., Koroteev, N. I., Zadkov, Yu. V., and Kruglik, S. G., Eds.).
21. Dzhagarov, B. M., Kruk, N. N., Tikhomirov, S. A., Gulbinas, V., and Andreyuk, G. M. (1994) Laser picosecond and nanosecond flash-photolysis of hemoglobin: excited states spectra and life-times, oxygen photodissociation and recombination, the pH-effect, *Lith. J. Phys. 34*, 108−113.
22. Frauenfelder, H., Sligar, S. G., and Wolynes, P. G. (1991) The energy landscape and motions of proteins, *Science 254*, 1598−1603.
23. Sawicki, C. A., and Gibson, Q. H. (1976) Quaternary changes in human hemoglobin studied by laser photolysis of carboxyhemo-globin, *J. Biol. Chem. 251*, 1533−1542.
24. Murray, L. P., Hofrichter, J., Henry, E. R., and Eaton, W. A. (1988) Time-resolved optical spectroscopy and structural dynamics following photodissociation of carbonmonoxyhemoglobin, *Biophys. Chem. 29*, 63−76.
25. Petrich, J. W., Lambry, J.-C., Kuczera, K., Karplus, M., Poyart, C., and Martin, J.-L. (1991) Ligand binding and protein relaxation in heme proteins: a room-temperature analysis of NO recombi-naiton, *Biochemistry 30*, 3975−3987.
26. Gibson, Q. H., Olson, J. S., McKinnie, R. E., and Rohlfs, R. J. (1986) A kinetic description of ligand binding to sperm whale myoglobin, *J. Biol. Chem. 261*, 10228−10239.
27. Ansari, A., Jones, C. M., Henry, E. R., Hofrichter, J., and Eaton, W. A. (1994) Conformational relaxation and ligand binding in myoglobin, *Biochemistry 33*, 5128−5145.
28. Benesch, R. E., Benesch, R., Renthal, R. D., and Maeda, N. (1972) Affinity labeling of the polyphosphate binding site of hemoglobin, *Biochemistry 11*, 3576−3582.
29. Bucci, E., and Fronticelli, C. (1965) A new method for the preparation of α and β subunits of human hemoglobin, *J. Biol. Chem. 240*, 551−552.
30. Galievsky, V. A. (2000) Ph.D. Thesis, Institute of Molecular and Atomic Physics, Minsk, Belarus.
31. Jasny, J., Sepiol, J., Karpiuk, J., and Gilewsky, J. (1994) Nanosecond transient absorption spectrophotometer with dye laser probing and computer control, *Rev. Sci. Instrum. 65*, 3646−3652.
32. Sawicki, C. A., and Gibson, Q. H. (1976) Quaternary changes in human hemoglobin studied by laser photolysis of carboxyhemo-globin, *J. Biol. Chem. 251*, 1533−1542.
33. Noble, R. W., Gibson, Q. H., Brunori, M., Antonini, E., and Wyman, J. (1969) The rates of combination of the isolated chains

photodissociation from haem proteins on ultrafast recombination, *Photochem. Photobiol. 31*, 479−484.

of human hemoglobin with oxygen, *J. Biol. Chem. 244*, 3905–3908.

34. Ye, X., Demidov, A., and Champion, P. M. (2002) Measurements of the photodissociation quantum yields of MbNO and MbO$_2$ and the vibrational relaxation of the six-coordinate heme species, *J. Am. Chem. Soc. 124*, 5914–5924.

35. Petrich, J. W., and Martin, J.-L. (1989) Ultrafast absorption and Raman spectroscopy of hemoglobin, *Chem. Phys. 131*, 31–47.

36. Dzhagarov, B. M. (1999) Excited states, relaxation processes, and coordination reactions in the active centres of heme proteins, *J. Appl. Spectrosc. 66*, 479–482.

37. Franzen, S., Bohn, B., Poyart, C., and Martin, J. L. (1995) Evidence for the subpicosecond heme doming in hemoglobin and myoglobin: a time-resolved resonance Raman comparison of carbonmonoxy and deoxy species, *Biochemistry 34*, 1224–1237.

38. Austin, R. H., Beeson, K. W., Eisenstein, L., Frauenfelder, H., and Gunsalus, I. C. (1975) Dynamics of ligand binding to myoglobin, *Biochemistry 14*, 5355–5373.

39. Steinbach, P. J., Ansari, A., Berendzen, J., Braunstein, D., Chu, K., Cowen, B. R., Ehrenstein, D., Frauenfelder, H., Johnson, J. B., Lamb, D. C., Luck, S., Mourant, J. R., Nienhaus, G. U., Ormos, P., Philipp, R., Xie, A., and Young, R. D. (1991) Ligand binding to heme proteins: connection between dynamics and function, *Biochemistry 30*, 3988–4001.

40. Scott, E. E., Gibson, Q. H., and Olson, J. S. (2001) Mapping the pathways for O$_2$ entry into and exit from myoglobin, *J. Biol. Chem. 276*, 5177–5188.

41. Case, D. A., and Karplus, M. (1979) Dynamics of ligand binding to heme proteins, *J. Mol. Chem. 132*, 343–368.

BI034928Q